Molecular Therapy
Nucleic Acids
Original Article

mRNA-engineered mesenchymal stromal cells expressing CXCR2 enhances cell migration and improves recovery in IBD

Qiaojia Li,[1,2,5] Yufan Lian,[1,2,5] Yiwen Deng,[2,3] Jieying Chen,[2,3] Tao Wu,[1] Xinqiang Lai,[2,4] Bowen Zheng,[1] Chen Qiu,[1] Yanwen Peng,[2,3] Weiqiang Li,[2,3] Andy Peng Xiang,[2,3] Xiaoran Zhang,[2,3] and Jie Ren[1]

[1]Department of Medical Ultrasonic, The Third Affiliated Hospital, Sun Yat-Sen University, No. 600 Tianhe Road, Guangzhou 510630, China; [2]Center for Stem Cell Biology and Tissue Engineering, Key Laboratory for Stem Cells and Tissue Engineering, Ministry of Education, Sun Yat-Sen University, Guangzhou 510080, China; [3]Department of Hepatic Surgery and Liver Transplantation Center, The Third Affiliated Hospital, Organ Transplantation Institute, Sun Yat-Sen University, Guangzhou 510630, China; [4]Cardiovascular Department, The Eighth Affiliated Hospital, Sun Yat-sen University, Shenzhen, Guangdong 518033, China

SUMMARY

Mesenchymal stromal cells (MSCs) have shown significant heterogeneity in terms of therapeutic efficacy for inflammatory bowel disease (IBD) treatment, which may be due to an insufficient number of MSCs homing to the damaged tissue of the colon. Engineering MSCs with specific chemokine receptors can enhance the homing ability by lentiviral transduction. However, the unclear specific chemokine profile related to IBD and the safety concerns of viral-based gene delivery limit its application. Thus, a new strategy to modify MSCs to express specific chemokine receptors using mRNA engineering is developed to evaluate the homing ability of MSCs and its therapeutic effects for IBD. We found that CXCL2 and CXCL5 were highly expressed in the inflammatory colon, while MSCs minimally expressed the corresponding receptor CXCR2. Transient expression of CXCR2 in MSC was constructed and exhibited significantly enhanced migration to the inflamed colons, leading to a robust anti-inflammatory effect and high efficacy. Furthermore, the high expression of semaphorins7A on MSCs were found to induce the macrophages to produce IL-10, which may play a critical therapeutic role. This study demonstrated that the specific chemokine receptor *CXCR2* mRNA-engineered MSCs not only improves the therapeutic efficacy of IBD but also provides an efficient and safe MSC modification strategy.

INTRODUCTION

Inflammatory bowel diseases (IBD), including ulcerative colitis (UC) and Crohn's disease (CD), are chronic inflammatory diseases of the gastrointestinal tract mucosa.[1,2] The incidence and prevalence of IBD are increasing worldwide.[3] Patients with IBD mainly present with abdominal pain, diarrhea, mucinous blood stool, tenesmus, and abdominal mass and tend to develop the complications of intestinal obstruction and fistulae. The disease progresses with relapses and remission periods, often impairing social life. However, the therapeutic effects of the available medical treatment are not satisfactory, and the majority of patients eventually need surgery to remove the diseased bowel. This situation has spurred clinical interest in developing new approaches for effectively controlling IBD.

In recent years, mesenchymal stromal cells (MSCs) have shown therapeutic potency in treating IBD due to their easy isolation and expansion, multi-lineage differentiation, paracrine effects, and immunomodulatory activities.[4,5] Preclinical and clinical data from animal models and humans have demonstrated that MSC therapy is safe for treating IBD[6–8]; however, significant heterogeneity exists in terms of therapeutic efficacy.[9–11] Localized injection of MSCs in the fistula tract of the colon with complex anal fistula has shown promising outcomes; 50% and 56% of the patients achieved the combined remission at weeks 24 and 52, respectively. The anal fistula healing rate (complete closure) is up to 64% (27/42) at week 8, and all fistulas were closed 4 years after MSC therapy.[7,12–14] Conversely, although some Phase I trials confirm the safety of MSCs therapy, the intravenous injection of MSCs results in an unsatisfactory treatment effect, with 34%–40% achieving clinical remission; of these, 50% of IBD patients were aggravated, which may be due to the insufficient number of MSCs homing to targeted issues.[7–9] Although a local injection of MSCs can achieve high treatment efficiency, its application range is limited.[7] For the extensive inflammatory injury of IBD, the

Received 23 December 2020; accepted 13 July 2021;
https://doi.org/10.1016/j.omtn.2021.07.009.

[5]Senior author

Correspondence: Dr. Andy Peng Xiang, Center for Stem Cell Biology and Tissue Engineering, Sun Yat-Sen University, 74# Zhongshan 2nd Road, Guangzhou, China.
E-mail: xiangp@mail.sysu.edu.cn
Correspondence: Dr. Xiaoran Zhang, Center for Stem Cell Biology and Tissue Engineering, Sun Yat-Sen University, 74# Zhongshan 2nd Road, Guangzhou, China.
E-mail: bfsj01@126.com
Correspondence: Dr. Jie Ren, Department of Medical Ultrasonic, The Third Affiliated Hospital of Sun Yat-sen University, No. 600 Tianhe Road, Guangzhou, China.
E-mail: renj@mail.sysu.edu.cn

 © 2021 The Authors.
This is an open access article under the CC BY-NC-ND license (http://creativecommons.org/licenses/by-nc-nd/4.0/).

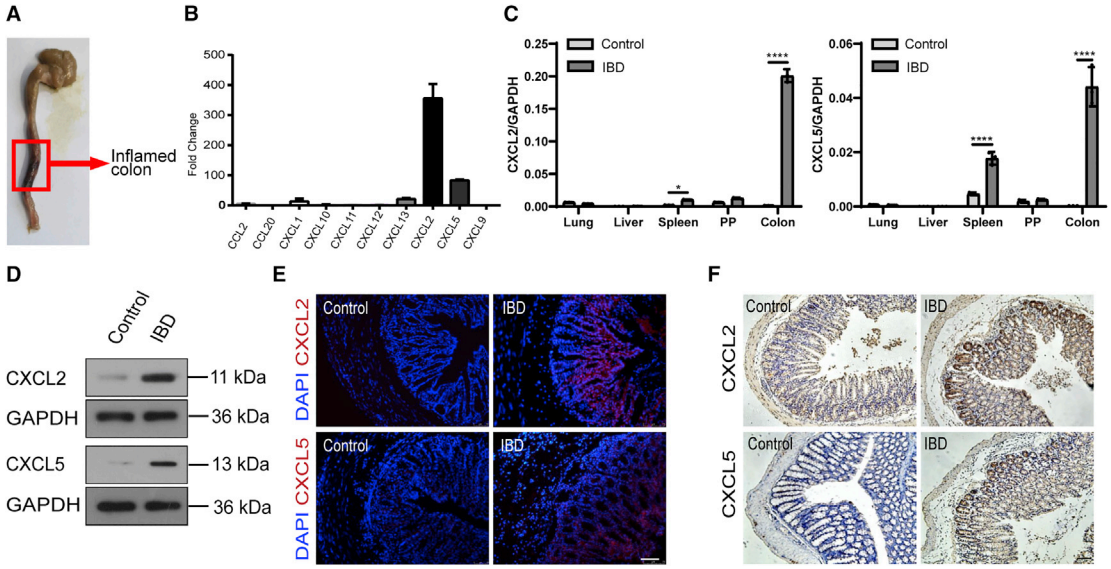

Figure 1. CXCL2 and CXCL5 expression in the inflamed colon of IBD mice

(A) The inflamed colon is indicated by the red box. (B) The mRNA extract from both control and IBD colon tissues was subjected to quantitative real-time PCR analysis. Various chemokines related to IBD inflammatory responses were analyzed. CXCL2 and CXCL5 showed significant change fold in the IBD colon compared to the control 24 h after challenge; n = 3. (C) The CXCL2 and CXCL5 expression in total tissue lysates of lungs, spleens, livers, and Peyer's patches (PP) from normal (control) and inflamed (IBD) as detected by quantitative real-time PCR. The experiment was repeated 3 times with tissues isolated from independent mice. (D) Mouse CXCL2 and CXCL5 expression in total tissue lysates from normal (control) and inflamed (IBD) colons as detected by western blotting. The experiment was repeated 3 times with tissues isolated from independent mice; a representative blot is shown. (E) Normal (control) and inflamed (IBD) colon sections were stained with CXCL2 (red) and CXCL5 (red) on day 1 post-challenge. Confocal images are representative of the results. The experiment was repeated 3 times with tissues isolated from independent mice. Nuclei were visualized by DAPI staining (blue). Scale bar, 75 μm. (F) Representative IHC images of normal (control) and inflamed (IBD) colon sections stained with anti-CXCL2 and anti-CXCL5 antibodies. The experiment was repeated 3 times with tissues isolated from independent mice; a representative image is shown. Scale bar, 75 μm. *$p < 0.05$, **$p < 0.01$, ***$p < 0.001$, ****$p < 0.0001$.

intravenous infusion is the convenient route for MSC administration. Therefore, it is necessary to develop a novel strategy for enhancing the homing ability of systemic infused MSCs for enhanced efficacy.

Furthermore, the right combination and interactions between the tissue-secreted chemokines and the corresponding chemokine receptors on MSCs play a vital role in homing to a specific (i.e., injured) tissue.[15,16] However, the chemokine receptors on MSCs are decreased significantly after *ex vivo* expansion, which markedly weakens the homing capacities of MSCs.[17] In previous studies, we demonstrated that engineering MSCs with specific chemokine receptors enhances the homing ability and improves the efficacy by lentiviral transduction-mediated overexpression of chemokine receptors.[18,19] Importantly, different types of injured organs secrete specific inflammatory cytokines and chemokines. Whether such a targeted strategy can improve the therapeutic efficacy of transplanted MSCs in IBD needs to be clarified.

Viral-based gene delivery has been widely used for the genetic engineering of MSCs.[20] This method is highly efficient, but limited by safety concerns, including insertional mutagenicity and potential immunogenicity of viral antigens. In addition, the relatively small transgene cargo capacity of viral systems and the time-consuming process are also considered to be constraints of the approach. Therefore, safe, transient, and efficient methods for genetic engineering of MSCs are highly desirable. The cytoplasmic delivery of mRNA in MSCs has gained attention because it is an integration-free method facilitating efficient expression of the transgene.[21]

Thus, in this study, we screen out disease-specific chemokines of IBD and genetically modify MSCs to express specific chemokine receptors using the mRNA-transfection system to evaluate the homing efficacy of MSCs and their therapeutic effects in a mouse model of IBD.

RESULTS

CXCL2 and CXCL5 are specific chemokines in the inflamed colon tissue of IBD mice

Since the chemokine-chemokine receptor axis is indispensable for MSC targeting, we examined the mRNA expression levels of various intestinal inflammation-related chemokines, such as *CCL2*, *CCL20*, *CXCL1*, *CXCL2*, *CXCL5*, and *CXCL9–13*, secreted by inflamed sites during IBD[22–24] (Figure 1A). Among these chemokines, CXCL2 and CXCL5 exhibit maximal changes at 24 h post-sensitization and were gradually decreased after 48 and 72 h, as compared to the normal colon (Figures 1B and S1A). We also detected the expression of CXCL2 and CXCL5 in lungs, livers, spleens, and Peyer's patches of

normal and IBD mice. The result was that CXCL2 and CXCL5 were significantly increased in the spleen and colon after sensitization; they were highest in the colon (Figure 1C). In addition, both western blotting (Figure 1D) and *in situ* immunohistochemistry (IHC) staining (Figures 1E and 1F) confirmed that CXCL2 and CXCL5 are dramatically upregulated in the inflamed colon.

mRNA synthesis and MSC transfection by electroporation

The combination of lesion-secreted chemokines and MSC-expressed receptors is crucial for targeting MSCs to inflamed tissues. Thus, we analyzed a set of common C-C and CXC motif chemokine receptors for their expression in MSCs cultured from three different donors. However, the mRNA levels of these chemokine receptors were drastically low in MSCs at the fourth passage (Figure 2A), including CXCR2 (Figure 2B), the most common chemokine receptor for both CXCL2 and CXCL5. The flow cytometry analysis also confirmed that the expression of CXCR2 in MSCs isolated from four independent donors was virtually undetectable (Figure 2C). The low-level expression of specific chemokine receptors on long-term culture human MSCs implied that MSCs may not efficiently home to the injured target tissue through the chemokine-chemokine receptor axis. Thus, it is necessary to improve the level of MSC-expressed CXCR2 to enhance the targeting abilities of MSCs for specific chemokines in IBD.

The delivery of mRNA by electroporation is a promising strategy to enhance receptor expression because it does not integrate into the genome and expresses transiently.[25,26] Considering these advantages, we examined whether mRNA transfection improves the expression of CXCR2 in MSCs via electroporation. We synthesized mRNA through an *in vitro* transcription reaction and bacterial amplification of the cDNA clones of both genes of interest: *CXCR2* and *EGFP*. Then mRNA was processed *in vitro* for 5′-capping and 3′-poly-adenylation to increase the stability and the translation efficiency (Figure S1B). A Kozak sequence was included to enhance the initiation signal for the translation of the proteins. Next, agarose gel electrophoresis confirmed that *CXCR2* and *EGFP* mRNAs were successfully synthesized (Figure S1C). Finally, MSCs transiently overexpressing EGFP alone (MSC^{EGFP}) or both CXCR2 and EGFP (CXCR2-MSC^{EGFP}) are generated by the introduction of corresponding mRNAs into the cells through electroporation.

CXCR2 and EGFP transient expression and safety following mRNA transfection

After MSC transfection with mRNA encoding *CXCR2* or *EGFP*, respectively, we tested the transfection efficiency. The CXCR2 expression was observed on day 1 post-transfection (Figure 2D), and flow cytometry demonstrated that >90% CXCR2-MSC^{EGFP} expressed CXCR2 (Figure 2E). This phenomenon declined gradually and finally disappeared on day 8 (Figures S2A–S2D). MSC^{EGFP} exhibited the same performance of transfection with CXCR2-MSC^{EGFP} (Figures 2D–2F). These outcomes demonstrated that electroporation not only achieved a high transfection efficiency but also accomplished a transient expression.

Next, we tested whether genetic manipulations altered the cell viability and the intrinsic characteristics of MSCs. In the aspect of cell viability, CCK8 assays demonstrated that the transfection of mRNA had no obvious effects on cell viability in CXCR2-MSC^{EGFP} or MSC^{EGFP} cells (Figure 2G). In addition, apoptosis experiments demonstrated that the rate of cell death is not altered significantly (Figures 2H and S3A). With respect to biological characteristics, flow cytometry analysis demonstrated that both MSC^{EGFP} and CXCR2-MSC^{EGFP} express the typical MSC marker profile (CD29, CD44, CD73, CD90, CD105, and CD166) and lack the expression of hematopoietic markers (CD34 and CD45; Figures S3B–S3D).

CXCR2-MSC^{EGFP} exhibits enhanced migration toward CXCL2 and CXCL5 *in vitro* and to inflamed colon *in vivo*

Next, we investigated whether the transient expression of CXCR2 increases the homing property of MSCs. At 24 h post-transfection, the cells were used in subsequent *in vitro* and *in vivo* experiments because CXCR2 protein showed the highest expression at this time point. *In vitro* transwell assays demonstrated a significantly high number of CXCR2-MSC^{EGFP} cells passing through the membrane pores in response to exogenous CXCL2/CXCL5 stimulation as compared to MSC^{EGFP} (Figures 3A and 3C). For *in vivo* chemotaxis assays, CXCR2-MSC^{EGFP} (1×10^6 per mouse) were injected into IBD mice through the tail vein at 24 h after colon sensitization. The distribution of MSCs was detected in the lungs, livers, spleens, Peyer's patches, and colons of mice by immunofluorescence. At 12 h post-injection, the numbers of MSCs in the lungs, livers, and spleens of mice did not differ significantly between MSC^{EGFP} and CXCR2-MSC^{EGFP} groups, while a significantly larger number of CXCR2-MSC^{EGFP} accumulated in the colons of IBD mice as compared to MSC^{EGFP} (12.00 ± 2.00 versus 3.00 ± 1.00 cell/field, $p < 0.001$; Figures 3B, 3D, and 3F).

To clarify whether the cells have migrated across the endothelium or are simply trapped within the intravascular space, we used CD31 (red) label the vessels to observe the location of MSCs (green). Immunohistochemistry showed that most MSCs were present in tissues rather than in vessels (Figure 3E).

Collectively, these results demonstrated that *CXCR2*-mRNA-modified MSCs specifically migrated to the inflamed colon, rather than to other organs or tissue *in vivo*, in response to CXCL2 and CXCL5 released from the damaged tissue of the colon.

Local enrichment of CXCR2-MSC^{EGFP} significantly improves IBD symptoms

To verify the therapeutic effects of CXCR2-MSC^{EGFP} treatment, a series of evaluations were performed to assess therapeutic outcomes. Gross images demonstrated that reduced colon length post-sensitization was remarkably reversed by CXCR2-MSC^{EGFP} infusion as compared to the MSC^{EGFP} and IBD groups (7.43 ± 0.40 versus 6.13 ± 0.35 versus 5.53 ± 0.50, $p < 0.01$) (Figures 4A and 4B). Relative body weight loss was recovered more quickly in CXCR2-MSC^{EGFP}-treated mice than that in the MSC^{EGFP} group at 3 days post-injection (1.06 ± 0.03 versus 0.97 ± 0.02, $p < 0.05$; Figure 4C). Moreover,

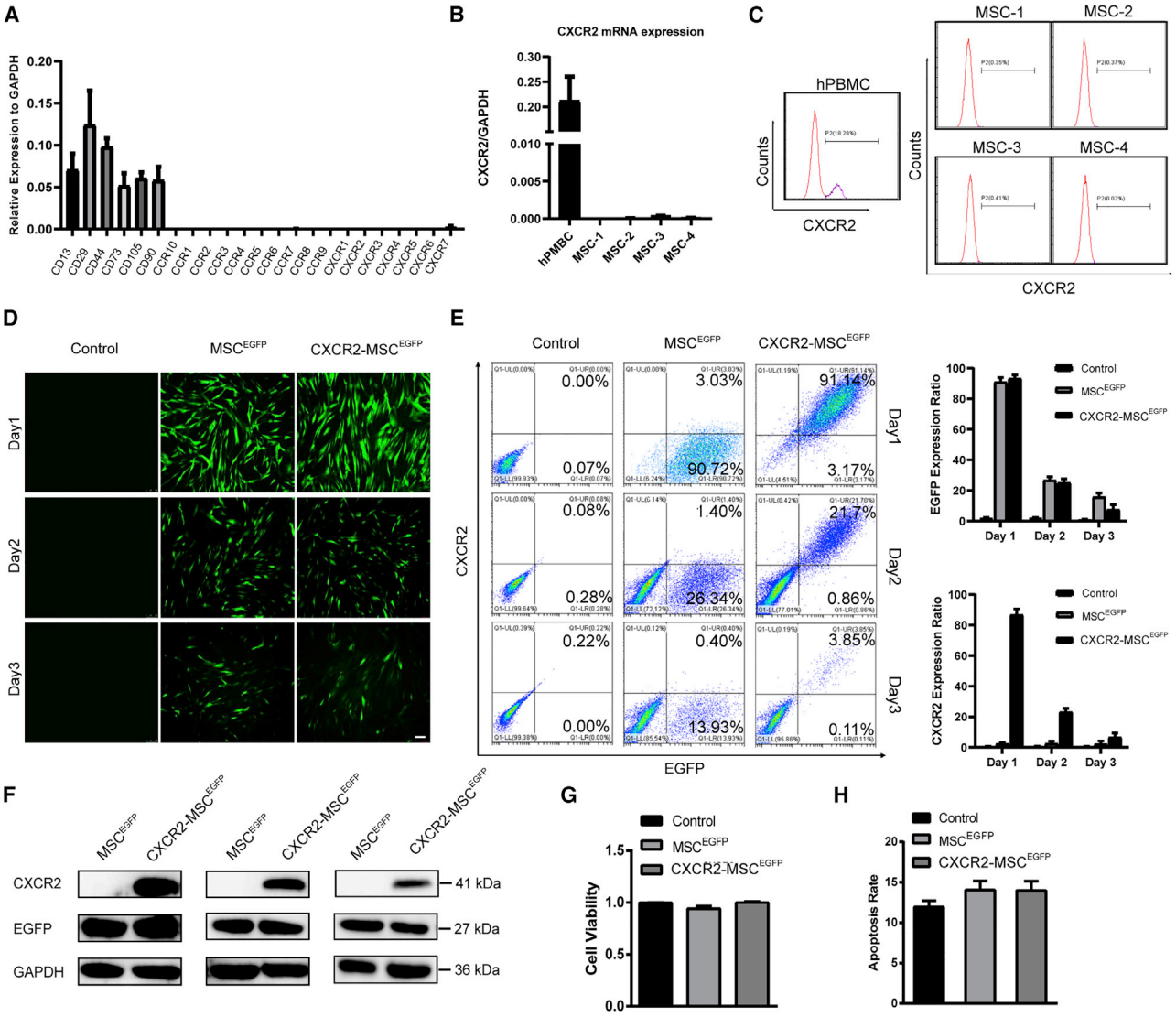

Figure 2. *CXCR2*-mRNA preparation and expression

(A) Histograms represent the mRNA expression profiles of CC and CXC chemokine receptors on the fourth passage of MSCs from 3 independent donors (mean ± SD). MSC surface markers including CD13, CD29, CD44, CD73, CD105, and CD90 served as positive controls (n = 3). (B) *CXCR2* mRNA expression levels in MSCs and Human peripheral blood mononuclear cells (hPBMCs) (positive control, mean ± SD). Glyceraldehyde 3-phosphate dehydrogenase gene (*GAPDH)* serves as an internal mRNA control. (C) The CXCR2 protein on the cell surface of MSCs from 4 independent donors was analyzed by flow cytometry. hPBMCs served as a positive control. All of the experiments were repeated at least 3 times. (D) MSCs were transduced with the *EGFP*-mRNA alone or with *CXCR2*-mRNA. Representative fluorescence images for MSC^{EGFP} and CXCR2-MSC^{EGFP} are displayed for 1, 2, and 3 days post-transduction. Scale bar, 75 μm. (E) The levels of the EGFP and CXCR2 proteins on the surface of MSC^{EGFP} and CXCR2-MSC^{EGFP} cells at 1, 2, and 3 days after electroporation, respectively. The experiment was repeated 3 times. (F) CXCR2 and EGFP expression of MSC^{EGFP} and CXCR2-MSC^{EGFP} at 1, 2, and 3 days after electroporation were confirmed by western blotting. The experiment was performed 3 times with cell lysates from MSCs; a representative blot is shown. (G) CCK-8 assay was used to determine cell viability. The experiments were repeated 3 times. (H) Annexin V and propidium iodide staining were used to determine cell apoptosis. The experiments were repeated 3 times.

CXCR2-MSC^{EGFP} led to a notable improvement in disease activity indexes in comparison to that of MSC^{EGFP} (4.00 ± 1.00 versus 1.67 ± 0.58, $p < 0.05$; Figure 4D). The morphology of colons was examined by ultrasound (Figure 4E). Furthermore, we found that the general structure of the colon after CXCR2-MSC^{EGFP} engraftment was similar to that of the normal group, whereas MSC^{EGFP} only slightly reduced mucosa thickening and luminal stenosis versus the IBD group (Figures 4F and 4G).

Histological examination demonstrated that IBD mice suffer from destruction of the entire epithelium, including severe submucosal edema, scattered infiltration of lamina propria, and submucosal

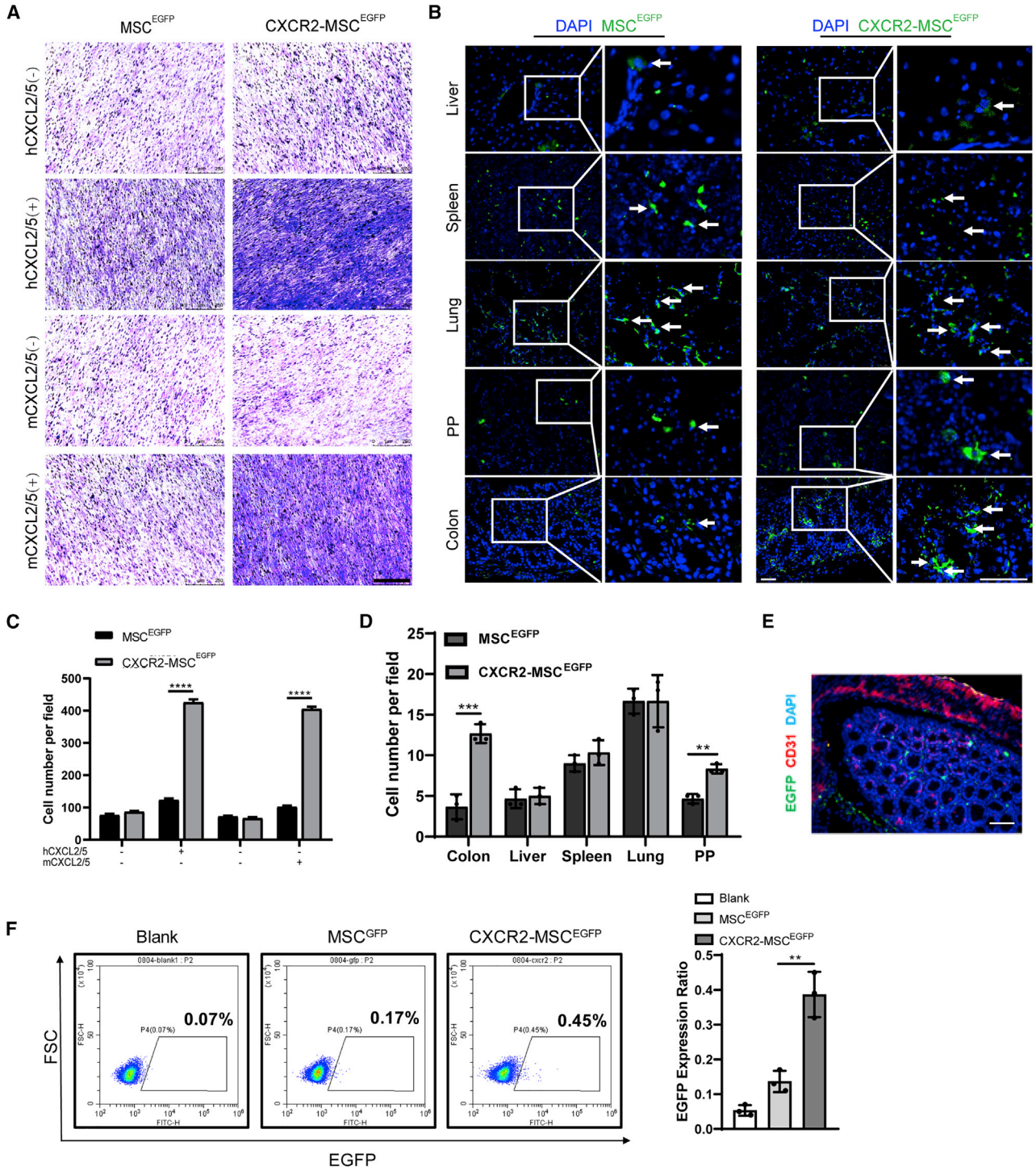

Figure 3. CXCR2-MSC^{EGFP} exhibits enhanced migration toward hCXCL2/hCXCL5 and mCXCL2/mCXCL5 *in vitro* and to inflamed colons *in vivo*

(A) *In vitro* migration of CXCR2-MSC^{EGFP} and MSC^{EGFP} toward human CXCL2 and CXCL5 (hCXCL2/hCXCL5) or murine CXCL2 and CXCL5 (mCXCL2/mCXCL5) was assessed by transwell invasion assays. Scale bar, 250 μm. (B) MSC^{EGFP} and CXCR2-MSC^{EGFP} were intravenously injected into IBD mice. Representative confocal images of EGFP-expressing MSCs at 12 h post-injection in the liver, spleen, lung, PP, and colon are displayed. Signals: EGFP, green; DAPI, blue. Scale bar, 25 μm. (C) *In vitro* cell

(legend continued on next page)

inflammatory cells. Compared to IBD mice, MSC^{EGFP} transplantation partially alleviated the mucosal destruction and edema in submucosa, while a significantly decreased histological score was observed in the CXCR2-MSC^{EGFP} group (Figure 5A). Because myeloperoxidase (MPO) activity reflects the degree of neutrophil infiltration, it may be used as an index for evaluating the severity of IBD,[27] and thus, examining the MPO activity of the damaged tissue of the colon. Compared to the control group, MPO activity was notably decreased in the CXCR2-MSC^{EGFP} group and differed slightly in the MSC^{EGFP} group (Figure 5B). These results proved that our modified CXCR2-MSC^{EGFP} could significantly improve the macro and micro symptoms of IBD.

Local increase in CXCR2-MSC^{EGFP} promotes M2 macrophages

To investigate the potential mechanism of CXCR2-MSC^{EGFP} in improving the symptoms of IBD, we used ELISA to measure the levels of anti-inflammatory (interleukin-10 [IL-10]) and pro-inflammatory (interferon-γ [IFN-γ], tumor necrosis factor-α [TNF-α], IL-12, IL-13, and IL-17) cytokines in the inflamed colon. The expression of pro-inflammatory cytokines in the inflamed colon of the CXCR2-MSC^{EGFP}-treated mice was significantly lower than those of the MSC^{EGFP}-treated group (Figure 5C). Conversely, the levels of IL-10 in the CXCR2-MSC^{EGFP}-treated group were much higher than those in the MSC^{EGFP}-treated group (43.98 ± 2.89 versus 38.14 ± 3.85, $p < 0.05$); also, the immunofluorescence examination obtained similar results (Figure 5D). These results suggested that CXCR2-MSC^{EGFP} exerts its therapeutic effects via anti-inflammatory mechanisms and pathways.

IBD is multifactorial chronic relapsing diseases involving a loss of balance between different types of T cells, resulting in the activation of macrophages as well as recruitment of circulating leukocytes into the gut, causing inflammation. Macrophages are reported to be key regulators of immune responses in the intestine and specifically promote tolerance in the gut.[28,29] Thus, we used flow cytometry to explore the correlation between T $CD4^+$ cells/macrophages and anti-inflammatory/pro-inflammatory cytokines. No significant differences were observed in T cells among four groups after MSC infusion (Figure 5E). However, we found that IL-10 produced by macrophages is significantly increased in the colons from the CXCR2-MSC^{EGFP}-treated group as compared to either the IBD or the MSC^{EGFP}-treated group (Figure 5F). This phenomenon suggested that the local increase in CXCR2- MSC^{EGFP} facilitated macrophages to produce more IL-10, and this may play a vital role in the treatment of IBD.

Putative mechanism of CXCR2-MSC^{EGFP} promoting macrophages to produce IL-10 in IBD

Macrophages play pivotal roles in the pathogenesis of IBD,[30,31] and MSCs can repolarize the pro-inflammatory M1 macrophages into anti-inflammatory M2 macrophages.[32,33] Therefore, we explored whether a large number of CXCR2-MSC^{EGFP} migrated to damaged tissue could affect macrophage functions and show obvious therapeutic effects against IBD *in vivo*. A genome-wide RNA sequencing (RNA-seq) analysis of MSCs derived from three different donors was conducted. The global transcriptional profiling data from these experiments were deposited in theSequence Read Archive (SRA) database of NCBI (accession number SRP095307). Semaphorins were the favorite assessment candidates in defining new regulatory molecules in various autoimmune or immune-mediated diseases. Semaphorins were understood to be frontline players in the field of immune responses.[34] Both increased and decreased semaphorins signaling has been linked to immune system diseases, especially in the intestinal mucosal immune system. Some investigators reported that the semaphorins were closely related to IBD. Just as the sema3E could attenuate intestinal inflammation,[34–36] the sema4D protect against colitis, and the serum levels of sema4A were significantly lower in patients with CD and UC when compared to those of the controls. We found that sema7A had the highest expression among all of the semaphorins identified in the MSCs (Figure 6A). Also, we found that the CXCR2 modification of MSCs with mRNA transfection did not change the expression of sema7A at the mRNA and protein levels (Figures 6B–6E). Since macrophages can bind semaphorin via an integrin receptor and lead to focal adhesion kinase (FAK) phosphorylation and mitogen-activated protein kinase (MAPK) activation with the subsequent release of the anti-inflammatory cytokine IL-10,[37] we postulated that some semaphorins exist in MSCs and may act as the activator of macrophage IL-10 production.

Next, we elucidated whether CXCR2-MSC^{EGFP} affected macrophage function via sema7A to improve IL-10 production *in vitro* and *in vivo*. When macrophages were cocultured with MSCs or a recombinant sema7A protein *in vitro*, the expression of IL-10 increased dramatically as compared to that of macrophages alone. To further verify the function of sema7A *in vivo*, we successfully suppressed the expression of sema7A in MSC using small molecular interfering RNA (siRNA) (Figures S4A and S4B). CCK8 assays demonstrated that the transfection of sema7A-siRNA had no obvious effects on cell viability in CXCR2-MSC^{EGFP} cells (Figure S4C). However, coculturing macrophages with MSCs with the siRNA-induced downregulation of sema7A expression produced little IL-10 (Figures 6F and 6G). To further verify a role for sema7A *in vivo*, inflamed colon sections were stained with specific antibodies (Figure S4D). These results indicated that most MSCs have overlapping sema7A staining and that abundant CXCR2-MSC^{EGFP} migrates to the inflamed colon and increases the production of IL-10 in comparison to MSC^{EGFP}.

Previous studies demonstrated that sema7A exerts its biological functions through the activation of FAK and, subsequently, ERK signaling pathways in immune cells.[38,39] Also, IL-10 production by macrophages

migration from (A) was quantified. Data are presented as means ± SDs. (D) Quantification of $EGFP^+$ cells per microscopic field of colon cryosections from (B). Data are presented as means ± SDs for each group. These data are representative of 3 independent experiments. (E) The colon sections were stained with human nuclei (green) and CD31 (red) on day 1 post-MSCs injection and representative confocal images were taken. Nuclei were visualized by DAPI staining (blue). Scale bar, 75 μm. (F) 12 h after MSC^{EGFP} and CXCR2-MSC^{EGFP} injection, cells from colon tissue were collected to detect the $EGFP^+$ cells by flow cytometric analysis. *$p < 0.05$, **$p < 0.01$, ***$p < 0.001$, ****$p < 0.0001$.

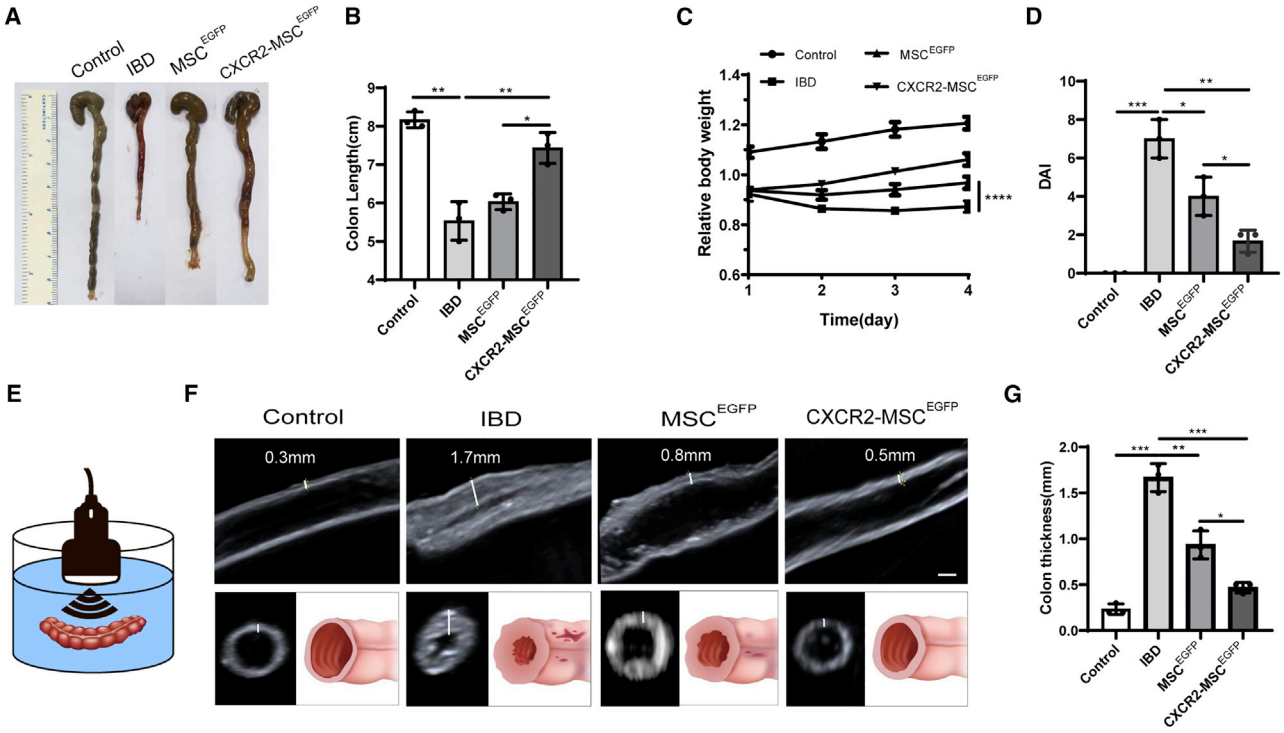

Figure 4. CXCR2-MSC^{EGFP} therapy alleviates IBD symptoms

(A) Control mice were challenged with 0.5% TNBS with prior sensitization. Experimental mice were intravenously (i.v.) injected with 1×10^6 CXCR2-MSC^{EGFP} or MSC^{EGFP} on day 1 of IBD. Representative photographs of colon samples from mice of each group are displayed. (B) Colon lengths from (A) were measured (n = 3 mice/group from 3 independent experiments). (C) Mice of each group were weighed from day 1 presensitization to 3 days post-sensitization (n = 3 mice/group from 3 independent experiments). (D) Disease activity index of colon tissues obtained from each group during IBD (72 h post-injection). Data are presented as means ± SDs for individual mice. (E) Schematic displaying the *in vitro* ultrasound imaging method for mouse colons. (F) Representative ultrasound images (longitudinal and cross-sections) of colon samples from mice for control and experimental groups. The white lines represent the thickness of the intestinal wall (n = 3 mice/group from 3 independent experiments). (G) Quantification of data from (F) is presented as means ± SDs for individual mice. *$p < 0.05$, **$p < 0.01$, ***$p < 0.001$.

is mediated by ERK signaling.[40] Consistent with these previous findings, the phosphorylation of FAK and ERK1/2 in macrophages cocultured with MSC or recombinant protein sema7A was observed (Figure S4E). Overall, macrophages interact with sema7A on MSCs and produce high levels of IL-10, which reduces inflammation.

CXCR2-MSC^{EGFP} exert therapeutic effects by sema7A

Compared to CXCR2-MSC^{EGFP}, colon length post-sensitization has no significant recovery by sema7A(−) CXCR2-MSC^{EGFP} injection (7.67 ± 0.15 versus 7.07 ± 0.31, $p < 0.01$) (Figures 7A and 7B). Relative body weight loss was recovered more slowly in sema7A(−) CXCR2-MSC^{EGFP}-treated mice than that in CXCR2-MSC^{EGFP} group at 3 days post-injection (1.01 ± 0.01 versus 1.04 ± 0.01, $p < 0.05$; Figure 7C). Moreover, sema7A(−) CXCR2-MSC^{EGFP} led to increased disease activity indexes in comparison to that of CXCR2-MSC^{EGFP} (5.33 ± 1.53 versus 1.67 ± 0.58, $p < 0.05$; Figure 7D). The pathological slices showed that the colons in the sema7A(−) CXCR2-MSC^{EGFP} group retain the mucosal destruction and edema, while a significantly decreased histological score was observed in the CXCR2-MSC^{EGFP} group (Figure 7E). At days 3, 5, and 7 after CXCR2-MSC^{EGFP} injection, the existence of human nuclei-positive cells in the colon tissue mean that MSCs may live for a period of time and play their roles (Figure S4F). These results show the important role of MSC-derived sema7A production in ameliorating disease activity.

DISCUSSION

In this study, using highly expressed chemokine ligands in the inflamed colon of the IBD model and mRNA transfection-engineered MSCs, we developed a novel approach for more efficient treatment of IBD, which is expected to be applicable for the clinical management of IBD. The mobilization of infused MSCs needs fine-tuned interaction between the chemokine ligands secreted by damaged tissues and the corresponding chemotactic receptors expressed on the surface of MSCs.[33] However, MSCs express limited chemokine receptors.[41] Wang et al.[42] increased the expression of chemokine receptors CXCR4 on MSCs for better efficacy of diabetic retinopathy. Unlike the common inflammation-related chemokine receptors, CXCL2 and CXCL5 are highly expressed in the inflamed colon of the IBD model and then established MSCs overexpressing CXCR2, the common receptor of CXCL2/CXCL5, which we demonstrated. CXCR2-overexpressing MSCs did exhibit high chemotactic activity and enhanced therapeutic effect, which was consistent with another study

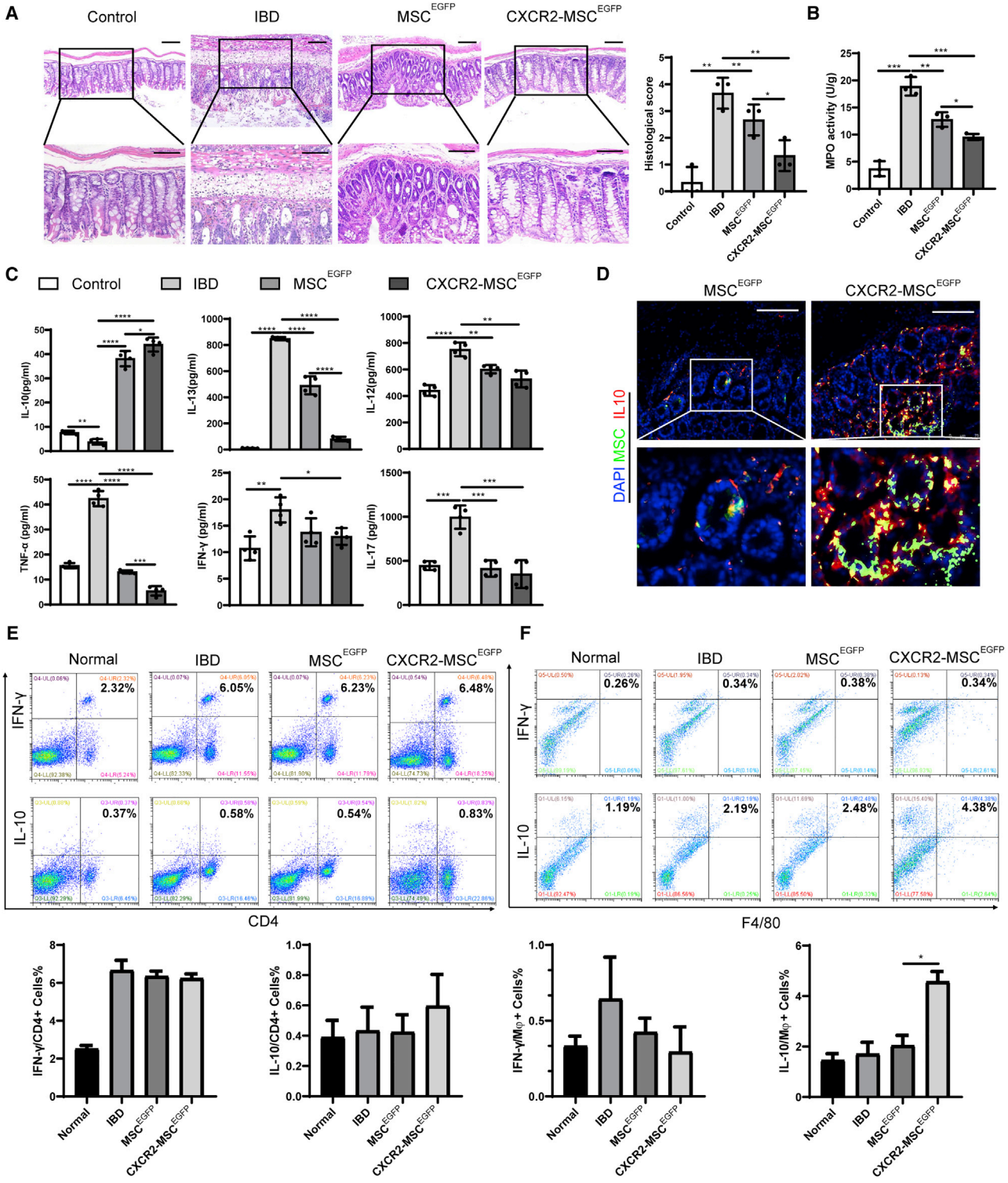

Figure 5. CXCR2-MSC^{EGFP} therapy reduces inflammatory response in IBD

(A) Representative H&E images of colon sections of control, IBD, MSC^{EGFP}-treated, and CXCR2-MSC^{EGFP}-treated mice at 24 h post-injection. Histopathological score of colon tissue from control, PBS-treated, MSC^{EGFP}-treated, and CXCR2-MSC^{EGFP}-treated mice is presented (right). Data are presented as means ± SDs for each group (n = 3 mice/group from 3 independent experiments). Scale bar, 100 μm. (B) MPO activity of colon tissue homogenates obtained from each group during TNBS-induced IBD (24 h

(legend continued on next page)

that CX3CL1 significantly upregulated in the inflamed colon tissues and the administration of the CX3CR1&IL-25-MSCs achieved a better therapeutic effect.[43] These results suggest that the study of IBD-specific chemokine factors is a more targeted approach for treatment and has certain reference significance for clinical treatment.

We found that non-CXCR2-transduced MSCs have a positive effect on colitis severity, although only a few end up in the colon. The therapeutic effects of MSCs partly rely on the capacity of MSCs to release trophic factors favoring tissue repair. A study found that MSCs can reduce colitis in mice via the release of TNF-α-stimulated gene-6 (TSG6).[44] MSCs also can produce pleiotropic gut trophic factors involved in each wound healing process, including the anti-inflammatory, proliferative, and tissue remodeling phases.[45] However, much research has demonstrated that the increased engraftment of MSCs at a specific site of interest has been shown to be very useful for treatment.[46,47] As expected, we demonstrated that more MSCs that expressed CXCR2 could respond positively to CXCL2 and CXCL5 and actively migrate to the damage site, thus improving the curative effect of IBD.

In terms of gene transfection, we selected the method of mRNA electroporation to engineer MSCs. Once mRNA has reached the cytoplasm, it is translated instantly. Conversely, DNA therapeutics need to access the nucleus to be transcribed into RNA, and their functionality depends on the nuclear envelope breakdown during cell division. In addition, mRNA is safer than DNA because it possesses the ability to transiently engineer cells without the risk of insertional mutagenesis. Chemical modification of mRNA provides effective, dose-dependent transient protein expression and reduces innate immunogenicity, which has been shown to be of great advantage in disease treatment. Ryser et al. engineered mesenchymal stem cells using mRNA transfection.[48] Moreover, Levy et al.[49] harnessed mRNA transfection to generate MSCs that simultaneously express functional rolling machinery PSGL-1 and SLeX. Furthermore, we transferred the IBD-specific chemokine receptors CXCR2 mRNA into MSCs by electroporation with excellent transfection efficiency (>90%). The encouraging data of mRNA-based genetic manipulations in MSC may translate into the clinic more advantageously than DNA modification.

IBD is a chronic relapsing disease due to the dysfunctional immune system. As mentioned in many studies, semaphorins are immunoregulatory molecules and play a protective role in IBD. Just as the sema3E could attenuate intestinal inflammation,[50] the sema4D protect against colitis[36]; the serum levels of sema4A were significantly lower in patients with CD and UC when compared to those of controls.[34] We found that sema7A, which is the gene with the highest expression on MSC in the semaphorins family, can stimulate macrophages in the colon to produce more IL-10, which was consistent with the research that sema7A was responsible for protective effects against colitis.[37] The more that CXCR2-MSC^{EGFP} migrate to the local tissue, the more macrophages were stimulated for abundant IL-10 and thus significantly improved the therapeutic effect, which suggests that sema7A may be a therapeutic target for IBD.

In summary, we performed *ex vivo* mRNA manipulation of MSCs and found that the overexpression of specific chemokine receptor CXCR2 enhances MSC homing to the inflamed tissue, thereby improving the treatment effect in the IBD mouse model. This method not only improves the therapeutic efficacy but it also provides an efficient and safe MSC modification strategy. Thus, it is possible that the strategy is also clinically applicable to other diseases.

Limitations of study

It cannot be ignored that there are some limitations to this study. Since the mRNA electrotransfection is a transient expression, we could not observe the survival of donor cells in colon tissues over longer periods. Human IBD is a chronic relapsing disease, and thus one administration of CXCR2-MSCs may be not enough. Additional studies are necessary to identify optimal CXCR2-MSCs doses and times, administration protocosl, and/or combination with other immunosuppressive agents to further improve the therapeutic effects.

MATERIALS AND METHODS

Mice

BALB/c male mice (6–8 weeks old) were purchased from the Animal Center of Sun Yat-sen University. All of the animal studies were carried out in accordance with the guidelines of the Sun Yat-sen University Institutional Animal Care and Use Committee.

Trinitrobenzenesulfonic acid (TNBS)-induced IBD in mice

First, the mice back skin (2 cm^2) were presensitized with TNBS on day 1. The presensitization solution was prepared by mixing acetone and olive oil in a 4:1 volume ratio by rigorous vortexing and then mixing 4 volumes of acetone/olive oil with 1 volume of 5% TNBS solution to obtain 1% (w/v) TNBS. The control mice were treated with the presensitization solution without TNBS. BALB/c mice were lightly anesthetized after a 24-h fast on day 8. To induce colitis, 5% TNBS (MilliporeSigma) in 50% ethanol (2.5 mg/kg TNBS) was administered intrarectally via a 3.5-French (F) catheter equipped with a 1-mL syringe. An anesthetized mouse was held by the tail, the catheter was inserted 4 cm into the anus, and 100 μL TNBS solution was injected into the rectum. The mouse should be held by the tail in a vertical position

post-injection) was examined by ELISA. Data are presented as means ± SDs for individual mice. (C) ELISA was used to measure the concentrations of IL-10, IFN-γ, IL-12, IL-13, TNF-α, and IL-17 in homogenates of colons obtained from each group 24 h post-injection. Data are presented as means ± SDs for each group (n = 3 mice/group from 3 independent experiments). (D) MSC^{EGFP} and CXCR2-MSC^{EGFP} were i.v. injected into IBD mice. Representative confocal images of colon sections after 3 days, are displayed. Signals: human nuclei, green; IL-10, red; DAPI, blue. Scale bar, 100 μm. (E) The percentages of IFN-γ/CD4$^+$ cells and IL-10/CD4$^+$ cells in colon tissues were measured by flow cytometry. The data are representative of 3 independent experiments. Quantifications are presented as means ± SDs. (F) The percentages of IFN-γ/macrophages and IL-10/macrophages in colon tissues were measured by flow cytometry. The data are representative of 3 independent experiments. Quantifications are presented as means ± SDs. *$p < 0.05$, **$p < 0.01$, ***$p < 0.001$, ****$p < 0.0001$.

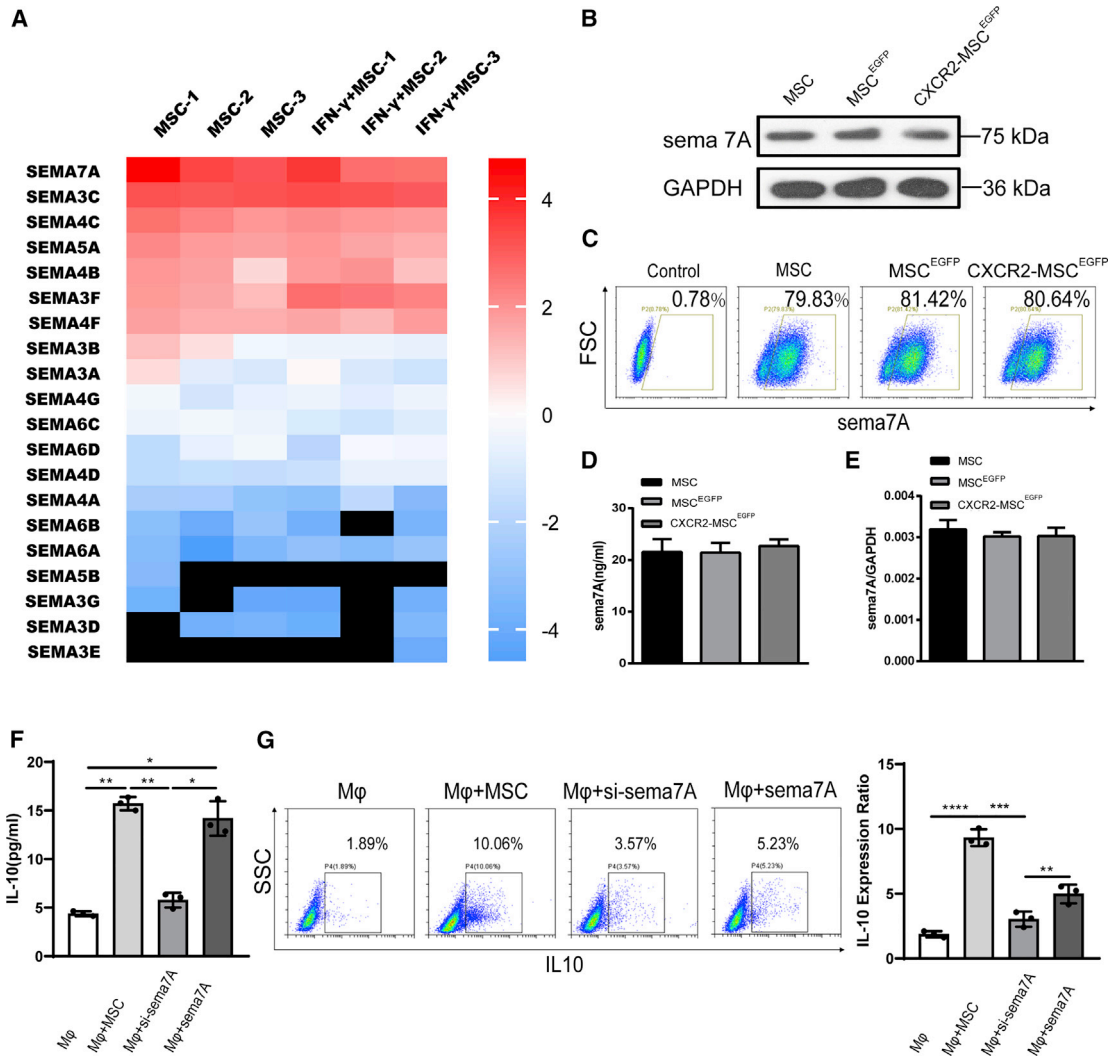

Figure 6. Possible mechanisms for CXCR2-MSC^{EGFP} alleviation of IBD.

(A) RNA-seq data analysis of MSCs from 6 donors (3 were stimulated by IFN-γ). The heatmap displays genes encoding semaphorin proteins. This heatmap was drawn with an RPKM value of log2. (B) Western blot displaying the expression of sema7A protein in MSC, MSC^{EGFP}, and CXCR2-MSC^{EGFP}; a representative blot is shown. (C) Flow cytometric analysis of sema7A protein on the cell surface of MSCs from the 3 mRNA groups. All of the experiments were repeated at least 3 times. (D) The culture medium from MSCs was collected; sema7A protein was detected by ELISA (means ± SDs). (E) *Sema7A* mRNA expression level in MSCs assessed by quantitative real-time PCR analysis (means ± SDs). *GAPDH* was used as an internal mRNA control. (F) Macrophages were co-cultured with MSCs, siRNA-sema7A MSCs, or 40 nM hsema7A. The culture media were used to detect dissociated IL-10 by ELISA. (G) Cells from (F) were collected to detect the intracellular level of IL-10 by flow cytometric analysis. *$p < 0.05$, **$p < 0.01$, ***$p < 0.001$, ****$p < 0.0001$.

with its head down for 2 min to allow uniform distribution of the TNBS solution.[51]

RNA isolation, reverse transcription, and quantitative real-time-PCR

Total RNA was extracted using an RNeasy mini kit (QIAGEN) according to the manufacturer's protocol. Reverse transcription was carried out using oligo-dT primers (Fermentas), and quantitative real-time PCR was performed using SYBR PCR Master Mix (Toyobo) according to the manufacturer's instructions. quantitative real-time PCR was conducted in duplicate for each sample, and three independent experiments were performed. The amplification signals were detected on a Light Cycler 480 detection system (Roche). The primer sequences are listed in Table S1.

Western blot analysis

Cell and colon tissue were lysed in 1× radioimmunoprecipitation assay (RIPA) buffer for western blot. The protein lysates were obtained by centrifugation at 15,000 × *g* for 5 min at 4°C. The total protein was separated by SDS-PAGE and transferred to a polyvinylidene

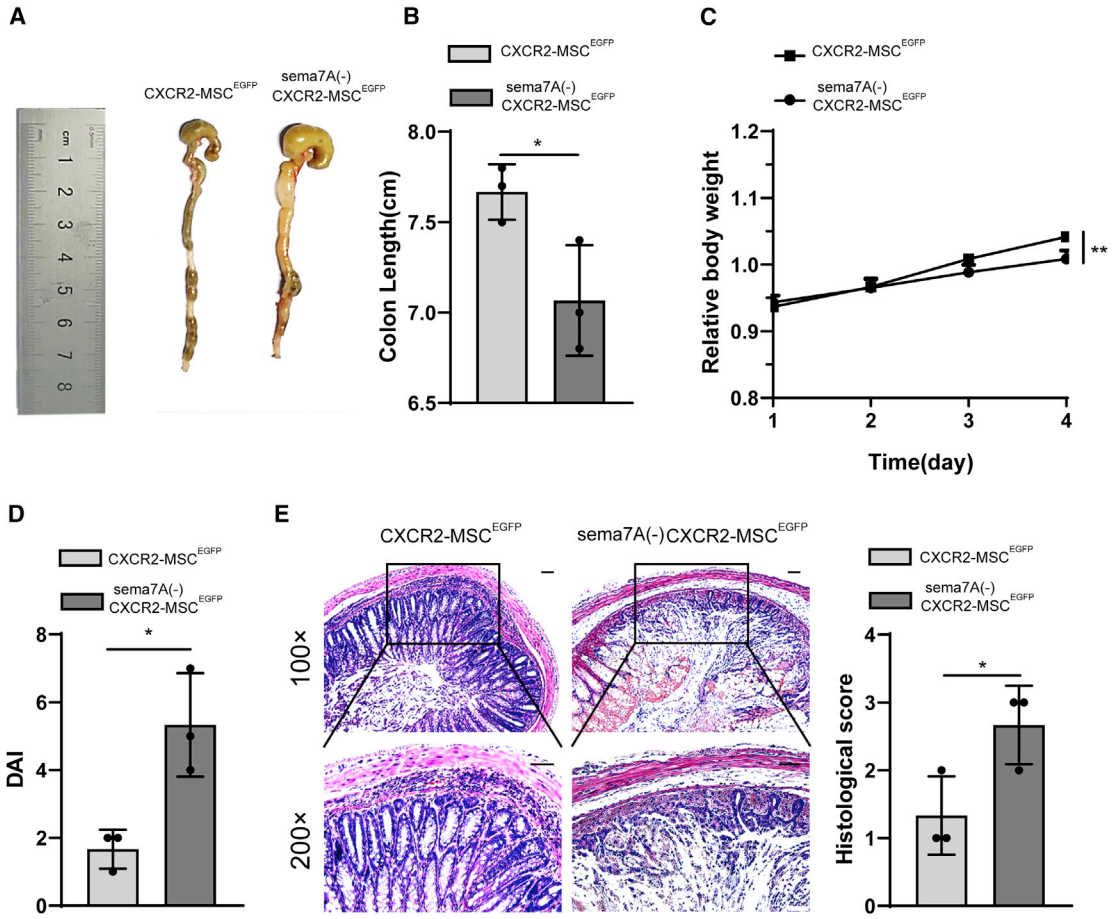

Figure 7. Sema7A(–) CXCR2-MSC^{EGFP} exert unsatisfactory therapeutic effect

(A) Experimental mice were i.v. injected with 1×10^6 CXCR2-MSC^{EGFP} or sema7A (–)CXCR2-MSC^{EGFP} on day 1 of IBD. Representative photographs of colon samples from the mice of each group are displayed. (B) Colon lengths from (A) were measured (n = 3 mice/group). (C) Mice of each group were weighed from day 1 presensitization to 3 days post-sensitization (n = 3 mice/group). (D) Disease activity index of colon tissues obtained from each group during IBD (72 h post-injection). Data are presented as means ± SDs for individual mice. (E) Representative H&E images of colon sections of CXCR2-MSC^{EGFP}-treated, and sema7A(–)CXCR2-MSC^{EGFP}-treated mice at 24 h post-injection. Histopathological scores of colon tissue from CXCR2-MSC^{EGFP}-treated and sema7A(–) CXCR2-MSC^{EGFP}-treated mice are presented here. Data are presented as means ± SDs for each group (n = 3 mice/group from 3 independent experiments). Scale bar, 100 μm. *$p < 0.05$, **$p < 0.01$, ***$p < 0.001$.

fluoride (PVDF) membrane (Millipore). The membrane was blocked with 5% BSA and probed with specific primary antibodies, followed by incubation with secondary antibodies at room temperature. The immunoreactive complexes were detected by enhanced chemiluminescence (GE Healthcare). The primary and secondary antibodies are listed in Table S2.

Immunofluorescence staining

At the indicated time points, colon tissues were harvested, fixed with 4% paraformaldehyde (Sigma), washed in phosphate-buffered saline (PBS), and dehydrated overnight in 30% sucrose (Sigma). Then, the samples were embedded in Tissue-Tek OCT compound (Bio-Optica) and frozen in an ethanol dry ice bath. Ten-nanometer-thick sections were placed on glass slides (Bio-Optica), blocked with 0.5% fetal bovine serum (FBS) in PBS-Tween 0.05% for 30 min, and then incubated with the appropriate primary and secondary antibodies overnight at 4°C and 30 min at room temperature, respectively. Nuclei were visualized with DAPI (Fluka). The images were acquired under fluorescence or confocal microscopy. The primary antibodies and secondary antibodies are listed in Table S2.

IHC staining

The colon samples of each group were immersed in 4% paraformaldehyde (PFA) and then embedded in paraffin. Sections were stained with streptavidin-biotin-peroxidase complex for IHC, and images were acquired by microscopy. The primary antibodies are listed in Table S2.

Isolation and characterization of MSCs

Human bone marrow samples were obtained from healthy donors, along with their informed consent. MSCs were isolated from the bone marrow and cultured as described previously.[52] In brief,

20–30 mL of bone marrow was diluted 1:1 with human MSC growth medium consisting of low-glucose DMEM (L-DMEM, HyClone) and 10% FBS (HyClone). Marrow mononuclear cells were separated by Ficoll-Paque (1.077 g/mL, Amersham Biosciences) density gradient centrifugation and seeded at a density of $1 \times 10^5/cm^2$ into T75 cell culture flasks. At 80% confluence, the cells were detached by 0.25% trypsin-EDTA and designated as passage 1. The cells were further passaged at a ratio of 1:3. The culture-expanded MSCs exhibited surface expression of CD29, CD44, CD73, CD90, CD105, and CD166 (MSC markers), but not CD34 or CD45 (hematopoietic markers). After the fourth passage, the multiple differentiation capacity of the MSCs was confirmed by their forced differentiation to osteoblasts, chondrocytes, or adipocytes, which was performed as described previously.[53–55]

Plasmid construct

The plasmid was constructed as described previously.[14] Briefly, the vectors pUp-EF1a, pDown-CXCR2, and pTail-IRES-EGFP were recombined into the pDest-puro vector using a recognized LR recombination reaction protocol described in the Gateway LR kit and a clonase enzyme mix (Invitrogen). The final lentiviral expression vector was designated pLV/puro-EF1a-CXCR2-IRES-EGFP (Figure S5A). Also, pLV/puro-EF1a-EGFP was constructed similarly (Figure S5B).

mRNA construction and transduction

Plasmid DNA was linearized with a restriction endonuclease cleavage downstream of the insert to be transcribed. The plasmid DNA containing a T7 RNA polymerase promoter site was used as a template for *in vitro* transcription with mMESSAGE mMACHINE T7 Ultra. Briefly, 10 μL of 2 × T7 NTP/ARCA, 2 μL 10 × T7 Reaction Buffer, 1 μg lincolon template DNA, 2 μL T7 Enzyme Mix, and nuclease-free water constituted a 20-μL reaction that was incubated at 37°C for 2 h. Then, T7 Ultra reaction, 36 μL nuclease-free water, 20 μL 5 × E-PAP buffer, 10 μL 25 mM $MnCl_2$, 10 μL ATP solution, and 4 μL E-PAP were added into the mixture and incubated at 37°C for 30–45 min to install poly(A) tailing. Finally, the reaction was stopped, RNA precipitated by adding 50 μL LiCl precipitation solution, and the mixture chilled for ≥30 min at −−20°C. Then, the RNA was precipitated by centrifugation at maximum speed for 15 min at 4°C. The pellet was washed again with 70% ethanol and resuspended in nuclease-free water to determine the concentration. At 80% confluency, MSCs were detached and resuspended in 400 μL Opti-MEM, followed by the addition of 10 μg of CXCR2 or EGFP mRNA into cell suspension and incubation on ice for 10 min. Finally, the mRNA was transduced into MSCs and cultured by the standard method.

Flow cytometry

MSCs and MSCs transduced with mRNA encoding human *CXCR2* and *EGFP* were incubated with the appropriate antibody in the dark at 4°C for 30 min and analyzed by flow cytometry using Influx (BD Biosciences) or Gallios (Beckman Coulter) flow cytometers. The data were analyzed using CytExpert software. The antibodies for flow cytometry are listed in Table S3. The experiment was carried out in triplicate.

Flow cytometric detection of apoptosis

At 24 h after electroporation, the MSC^{EGFP} and CXCR2-MSC^{EGFP} cells were digested by trypsin and washed with cold fluorescence-activated cell sorting (FACS) buffer (0.1% sodium azide and 0.5% BSA in PBS), and then stained for 15 min with annexin V and propidium iodide (PI) in the binding buffer according to the manufacturer's instructions. Flow cytometric analyses were performed on Influx, and the data were analyzed using CytExpert software.

Migration assays

Migration was assessed using a transwell chamber system of 8-mm pore membrane filters (PIEP12R48, Millipore). Each upper chamber was loaded with serum-starved MSCs (2×10^5/well), whereas each lower chamber was loaded with 500 μL serum-free medium with or without hCXCL2 and hCXCL5 (5 ng/mL, PeproTech) or mCXCL2 and mCXCL5 (50 ng/mL, PeproTech). After 5–10 h incubation at 37°C in 5% CO_2, the cells remaining on the upper surfaces were removed with a cotton wool swab, and the filters were fixed and stained with 0.1% crystal violet. The cells that had migrated to the lower surface were counted under a microscope.

MSC transplantation and *in vivo* distribution

Our experimental design consisted of four groups: control group, IBD group, MSC^{EGFP} group, and CXCR2-MSC^{EGFP} group. During the modeling process, ~8% of the mice died from either anesthesia or inflammation, and the dead mice were ruled out in the experiment and statistics. All of the injections were administered 24 h after sensitization, and the cells were suspended in a 0.1-mL medium via the tail vein. To detect the distribution of transplanted MSC^{EGFP} or CXCR2-MSC^{EGFP} *in vivo*, samples were collected from the colon of recipients at 12 h post-injection. Also, samples of the spleens, Peyer's patches, lungs, livers, and colons from the recipients were collected for cryosection. The sections were counterstained with 1.0 mg/mL DAPI in PBS for 20 min at room temperature in the dark.

Clinical disease score evaluation

Animals were monitored for the symptoms of diarrhea and body weight loss every day for 4 consecutive days. For disease activity, a clinical score system consisting of the percentage of weight loss, stool texture, degree of colonic inflammation, colon adhesion, and congestive colon was used. Such evaluation used a criterion score in which each signal exhibited by the animal corresponded to one point. Finally, the sum of all of the values for each animal was calculated and plotted to construct a graph.[56]

Ultrasound imaging

We harvested the colon tissue from the ileocecal region to anus for ultrasonic imaging. The feces were expelled and the colon was brimmed by enteral irrigation with physiological sodium chloride solution. The colon was immersed in saline and another senior doctor used a clinical ultrasound imaging system (SIEMENS) to observe

the form of the colon. The thickest segment of the colon wall was selected for the measurement of colon lumen size and wall thickness three times per mouse. The *in vitro* images were acquired using a 18L6 HD high-frequency scope with the following imaging parameters: GEN/15 MHz and 0Db/DR 70.

Histopathological analysis

For the histopathological analysis, a colon specimen from the middle part (4 cm to the anus) was fixed in 10% buffered formalin phosphate and then embedded in paraffin. The sections were stained with hematoxylin and eosin, and inflammation was graded from 0 to 4 in a blinded fashion as follows: 0, no signs of inflammation; 1, low leukocyte infiltration; 2, moderate leukocyte infiltration; 3, high leukocyte infiltration, moderate fibrosis, high vascular density, thickening of the colon wall, moderate goblet cell loss, and focal loss of crypts; and 4, transmural infiltrations, massive loss of goblet cells, extensive fibrosis, and diffuse loss of crypts.[57]

Measurement of MPO activity

For neutrophils, the MPO activity was evaluated in the colon samples. At 24 h after MSC injection, colon tissues were harvested, homogenized in 0.5% cetyltrimethylammonium chloride (Sigma-Aldrich), passed through a nylon mesh, and collected by centrifugation at 3,000 rpm for 20 min at 4°C. The MPO activity was assessed with the commercial kit (Cusabio, CSB-E08723m) according to the manufacturer's instructions, as expressed as the absorbance per gram of total protein in the colon tissue homogenate.

ELISA

The expression of IFN-γ, TNF-α, IL-10, IL-12, IL-13, and IL-17 (all from e-Bioscience) in the inflamed colon of each group was measured using commercial ELISA kits according to the manufacturer's protocols.

Detection of lymphocytes and macrophages from mouse colon

Mice were sacrificed and colons were removed and placed in PBS. The colon was opened longitudinally, washed in PBS, and cut into 0.5-cm pieces. The segments of the colon were digested for 30 min with continuous stirring at 37°C with collagenase IV (800 Mandl units/mL; Roche) in RPMI 1640 medium containing 5% (v/v) fetal calf serum (FCS). The tissue debris was removed through the filter screen, and the collected whole cells were used in assays. The cells were fixed; permeabilized; stained for cell surface markers CD3, CD4, F4/80, cytoplasmic TNF-α, and IL-10; and at least 30,000 cells were gated and analyzed by flow cytometry. We set gates according to the scattered light of cells to establish the interception range of lymphocytes (R1) and macrophages (R2), and then set gates for the cells in R1 and R2 according to the fluorescence parameters. The antibodies for flow cytometry are listed in Table S3.

Analysis of bulk RNA-seq

Bulk RNA-seq of MSCs treated with IFN-γ (20 ng/mL) or not was performed in our previous study,[58] which has been deposited in the Sequence Read Archive (SRA) database of National Center for Biotechnology Information (NCBI) (accession number SRP095307). Using the DAVID Gene Functional Classification Tool (https://david.ncifcrf.gov/) and Gene Ontology database, we explored the biological functions of genes and semaphorin genes were selected. Their reads per kilobase of transcript per million mapped reads (RPKM) values were performed log2-transformed and showed through heatmaps drawn with GraphPad Prism (version 8.0.1).

siRNAs for knockdown

In vitro silencing of sema7A in MSCs was performed using three sets of shSema7A.MSC (1×10^5 cells) cultured in 12-well plates overnight and transfected with 20 nM shsema7A-1, shsema7A-2, and shsema7A-3, respectively, using a commercial kit (Ribobio). At 24 h after transfection, the cell homogenates were extracted for western blot and qPCR:

shsema7A-1: GCATCCTGTTCATCGAGAA

shsema7A-2: CATGTGCTTTACCTAACTA

shsema7A-3: ACGCCATTGTTCCACTCTA

Isolation of macrophages from mouse colon

Mouse were sacrificed and their colons were removed and placed in PBS. The colon was slit lengthwise, washed with PBS, and cut into 0.5-cm pieces. Colon segments of digestion for 30 min in collagenase IV 37°C. The pieces were treated for 30 min at 37°C with PBS containing 5% (v/v) FCS, HEPES (20 nM) (pH 7.4), penicillin (100 U/mL), streptomycin (100 U/mL), sodium pyruvate (1 mM), EDTA (10 mM), and polymyxin B (10 mg/mL; Calbiochem) to remove the epithelial cells and then were washed extensively with PBS. Segments of the colon were digested for 45 min with continuous stirring at 37°C, with collagenase D (800 Mandl units/mL; Roche), DNase I (10 mg/mL; Roche), and dispase I (10 mg/mL; Invitrogen) in RPMI 1640 medium with 5% (v/v) FCS. EDTA was added (final concentration, 10 mM), and cell suspensions were incubated for an additional 5 min at 37°C. Cells were spun through a 17.5% (w/v) solution of Accudentz (Accurate Chemical & Scientific), and collected whole cells were used in assays. Macrophages were sorted on the basis of their expression of F4/80, CD11b with an FACSAria (BD Biosciences).

Coculture of MSCs and macrophages and measurement of IL-10 production by macrophages

Mouse macrophages were cultured in 12-well plates alone or cocultured with MSCs with direct cell-cell contact (5:1 ratio), sisema7A-MSCs (5:1 ratio), or recombinant sema7A protein (R&D Systems, 2068-S7-050). After 72 h post-transduction, the macrophages were stained for cell surface F4/80 and cytoplasmic IL-10, and evaluated by flow cytometry (BD Biosciences PharMingen). The specific antibodies are listed in Table S3.

Statistical analysis

All of the data are presented as means ± SDs from at least three independent experiments. One-way analysis of variance (ANOVA) and t test were used to compare mean responses among the treatments. All

of the statistical analyses were performed using SPSS version 14.0 (SPSS, Chicago, IL, USA). $p < 0.05$ (*) was considered significant.

SUPPLEMENTAL INFORMATION

Supplemental information can be found online at https://doi.org/10.1016/j.omtn.2021.07.009.

ACKNOWLEDGMENTS

This work was supported by the National Key Research and Development Program of China, Stem Cell and Translational Research (2017YFA0103802), the National Natural Science Foundation of China (81971632 and 81900075), the Natural Science Foundation of Guangdong Province (2015A030312013, 2020A1515010425, and 2021A1515011759), the Key Scientific and Technological Projects of Guangdong Province (2017B020231001, 2018B030332001, and 2019B020235002), and the Key Scientific and Technological Program of Guangzhou City (201604020132 and 201802020023).

AUTHOR CONTRIBUTIONS

Conceptualization, J.R., A.P.X., and X.Z.; methodology, Q.L., Y.L., and Y.D.; investigation, X.Z., Y.D., J.C., T.W., and X.L.; writing – original draft, Q. L., Y. L., and X.Z.; writing – review & editing, A.P.X. and J.R.; funding acquisition, B.Z., C.Q., and Y.P.; resources, J.R. and W.L.; supervision, A.P.X. and J.R.

DECLARATION OF INTERESTS

The authors declare no competing interests.

REFERENCES

1. Kappelman, M.D., Rifas-Shiman, S.L., Porter, C.Q., Ollendorf, D.A., Sandler, R.S., Galanko, J.A., and Finkelstein, J.A. (2008). Direct health care costs of Crohn's disease and ulcerative colitis in US children and adults. Gastroenterology *135*, 1907–1913.
2. Hanauer, S.B. (2006). Inflammatory bowel disease: epidemiology, pathogenesis, and therapeutic opportunities. Inflamm. Bowel Dis. *12* (*Suppl 1*), S3–S9.
3. Kaplan, G.G. (2015). The global burden of IBD: from 2015 to 2025. Nat. Rev. Gastroenterol. Hepatol. *12*, 720–727.
4. Salem, H.K., and Thiemermann, C. (2010). Mesenchymal stromal cells: current understanding and clinical status. Stem Cells *28*, 585–596.
5. Barzilay, R., Melamed, E., and Offen, D. (2009). Introducing transcription factors to multipotent mesenchymal stem cells: making transdifferentiation possible. Stem Cells *27*, 2509–2515.
6. Lanzoni, G., Alviano, F., Marchionni, C., Bonsi, L., Costa, R., Foroni, L., Roda, G., Belluzzi, A., Caponi, A., Ricci, F., et al. (2009). Isolation of stem cell populations with trophic and immunoregulatory functions from human intestinal tissues: potential for cell therapy in inflammatory bowel disease. Cytotherapy *11*, 1020–1031.
7. Panés, J., García-Olmo, D., Van Assche, G., Colombel, J.F., Reinisch, W., Baumgart, D.C., Dignass, A., Nachury, M., Ferrante, M., Kazemi-Shirazi, L., et al.; ADMIRE CD Study Group Collaborators (2016). Expanded allogeneic adipose-derived mesenchymal stem cells (Cx601) for complex perianal fistulas in Crohn's disease: a phase 3 randomised, double-blind controlled trial. Lancet *388*, 1281–1290.
8. Duijvestein, M., Vos, A.C., Roelofs, H., Wildenberg, M.E., Wendrich, B.B., Verspaget, H.W., Kooy-Winkelaar, E.M., Koning, F., Zwaginga, J.J., Fidder, H.H., et al. (2010). Autologous bone marrow-derived mesenchymal stromal cell treatment for refractory luminal Crohn's disease: results of a phase I study. Gut *59*, 1662–1669.
9. Dhere, T., Copland, I., Garcia, M., Chiang, K.Y., Chinnadurai, R., Prasad, M., Galipeau, J., and Kugathasan, S. (2016). The safety of autologous and metabolically fit bone marrow mesenchymal stromal cells in medically refractory Crohn's disease - a phase 1 trial with three doses. Aliment. Pharmacol. Ther. *44*, 471–481.
10. Qiu, Y., Li, M.Y., Feng, T., Feng, R., Mao, R., Chen, B.L., He, Y., Zeng, Z.R., Zhang, S.H., and Chen, M.H. (2017). Systematic review with meta-analysis: the efficacy and safety of stem cell therapy for Crohn's disease. Stem Cell Res. Ther. *8*, 136.
11. Forbes, G.M., Sturm, M.J., Leong, R.W., Sparrow, M.P., Segarajasingam, D., Cummins, A.G., Phillips, M., and Herrmann, R.P. (2014). A phase 2 study of allogeneic mesenchymal stromal cells for luminal Crohn's disease refractory to biologic therapy. Clin. Gastroenterol. Hepatol. *12*, 64–71.
12. Panés, J., García-Olmo, D., Van Assche, G., Colombel, J.F., Reinisch, W., Baumgart, D.C., Dignass, A., Nachury, M., Ferrante, M., Kazemi-Shirazi, L., et al.; ADMIRE CD Study Group Collaborators (2018). Long-term Efficacy and Safety of Stem Cell Therapy (Cx601) for Complex Perianal Fistulas in Patients With Crohn's Disease. Gastroenterology *154*, 1334–1342.e4.
13. Lee, W.Y., Park, K.J., Cho, Y.B., Yoon, S.N., Song, K.H., Kim, D.S., Jung, S.H., Kim, M., Yoo, H.W., Kim, I., et al. (2013). Autologous adipose tissue-derived stem cells treatment demonstrated favorable and sustainable therapeutic effect for Crohn's fistula. Stem Cells *31*, 2575–2581.
14. Barnhoorn, M.C., Wasser, M.N.J.M., Roelofs, H., Maljaars, P.W.J., Molendijk, I., Bonsing, B.A., Oosten, L.E.M., Dijkstra, G., van der Woude, C.J., Roelen, D.L., et al. (2020). Long-term Evaluation of Allogeneic Bone Marrow-derived Mesenchymal Stromal Cell Therapy for Crohn's Disease Perianal Fistulas. J. Crohn's Colitis *14*, 64–70.
15. Sordi, V. (2009). Mesenchymal stem cell homing capacity. Transplantation *87* (9, Suppl), S42–S45.
16. Chamberlain, G., Fox, J., Ashton, B., and Middleton, J. (2007). Concise review: mesenchymal stem cells: their phenotype, differentiation capacity, immunological features, and potential for homing. Stem Cells *25*, 2739–2749.
17. Rombouts, W.J., and Ploemacher, R.E. (2003). Primary murine MSC show highly efficient homing to the bone marrow but lose homing ability following culture. Leukemia *17*, 160–170.
18. Zhang, X., Huang, W., Chen, X., Lian, Y., Wang, J., Cai, C., Huang, L., Wang, T., Ren, J., and Xiang, A.P. (2017). CXCR5-Overexpressing Mesenchymal Stromal Cells Exhibit Enhanced Homing and Can Decrease Contact Hypersensitivity. Mol. Ther. *25*, 1434–1447.
19. Huang, Y., Wang, J., Cai, J., Qiu, Y., Zheng, H., Lai, X., Sui, X., Wang, Y., Lu, Q., Zhang, Y., et al. (2018). Targeted homing of CCR2-overexpressing mesenchymal stromal cells to ischemic brain enhances post-stroke recovery partially through PRDX4-mediated blood-brain barrier preservation. Theranostics *8*, 5929–5944.
20. Ullah, M., Liu, D.D., and Thakor, A.S. (2019). Mesenchymal Stromal Cell Homing: Mechanisms and Strategies for Improvement. iScience *15*, 421–438.
21. Sahin, U., Karikó, K., and Türeci, Ö. (2014). mRNA-based therapeutics–developing a new class of drugs. Nat. Rev. Drug Discov. *13*, 759–780.
22. Puleston, J., Cooper, M., Murch, S., Bid, K., Makh, S., Ashwood, P., Bingham, A.H., Green, H., Moss, P., Dhillon, A., et al. (2005). A distinct subset of chemokines dominates the mucosal chemokine response in inflammatory bowel disease. Aliment. Pharmacol. Ther. *21*, 109–120.
23. Trivedi, P.J., and Adams, D.H. (2018). Chemokines and Chemokine Receptors as Therapeutic Targets in Inflammatory Bowel Disease; Pitfalls and Promise. J. Crohn's Colitis *12*, 1508.
24. Koelink, P.J., Overbeek, S.A., Braber, S., de Kruijf, P., Folkerts, G., Smit, M.J., and Kraneveld, A.D. (2012). Targeting chemokine receptors in chronic inflammatory diseases: an extensive review. Pharmacol. Ther. *133*, 1–18.
25. Beatty, G.L., Haas, A.R., Maus, M.V., Torigian, D.A., Soulen, M.C., Plesa, G., Chew, A., Zhao, Y., Levine, B.L., Albelda, S.M., et al. (2014). Mesothelin-specific chimeric antigen receptor mRNA-engineered T cells induce anti-tumor activity in solid malignancies. Cancer Immunol. Res. *2*, 112–120.
26. Kah, J., Koh, S., Volz, T., Ceccarello, E., Allweiss, L., Lütgehetmann, M., Bertoletti, A., and Dandri, M. (2017). Lymphocytes transiently expressing virus-specific T cell receptors reduce hepatitis B virus infection. J. Clin. Invest. *127*, 3177–3188.
27. Eeckhaut, V., Machiels, K., Perrier, C., Romero, C., Maes, S., Flahou, B., Steppe, M., Haesebrouck, F., Sas, B., Ducatelle, R., et al. (2013). Butyricicoccus pullicaecorum in inflammatory bowel disease. Gut *62*, 1745–1752.

28. Grégoire, C., Lechanteur, C., Briquet, A., Baudoux, É., Baron, F., Louis, E., and Beguin, Y. (2017). Review article: mesenchymal stromal cell therapy for inflammatory bowel diseases. Aliment. Pharmacol. Ther. *45*, 205–221.

29. Scott, N.A., Andrusaite, A., Andersen, P., Lawson, M., Alcon-Giner, C., Leclaire, C., Caim, S., Le Gall, G., Shaw, T., Connolly, J.P.R., et al. (2018). Antibiotics induce sustained dysregulation of intestinal T cell immunity by perturbing macrophage homeostasis. Sci. Transl. Med. *10*, eaao4755.

30. Bain, C.C., and Mowat, A.M. (2014). Macrophages in intestinal homeostasis and inflammation. Immunol. Rev. *260*, 102–117.

31. Zigmond, E., Bernshtein, B., Friedlander, G., Walker, C.R., Yona, S., Kim, K.W., Brenner, O., Krauthgamer, R., Varol, C., Müller, W., and Jung, S. (2014). Macrophage-restricted interleukin-10 receptor deficiency, but not IL-10 deficiency, causes severe spontaneous colitis. Immunity *40*, 720–733.

32. Németh, K., Leelahavanichkul, A., Yuen, P.S., Mayer, B., Parmelee, A., Doi, K., Robey, P.G., Leelahavanichkul, K., Koller, B.H., Brown, J.M., et al. (2009). Bone marrow stromal cells attenuate sepsis via prostaglandin E(2)-dependent reprogramming of host macrophages to increase their interleukin-10 production. Nat. Med. *15*, 42–49.

33. Manferdini, C., Paolella, F., Gabusi, E., Gambari, L., Piacentini, A., Filardo, G., Fleury-Cappellesso, S., Barbero, A., Murphy, M., and Lisignoli, G. (2017). Adipose stromal cells mediated switching of the pro-inflammatory profile of M1-like macrophages is facilitated by PGE2: in vitro evaluation. Osteoarthritis Cartilage *25*, 1161–1171.

34. Vadasz, Z., Rainis, T., Nakhleh, A., Haj, T., Bejar, J., Halasz, K., and Toubi, E. (2015). The Involvement of Immune Semaphorins in the Pathogenesis of Inflammatory Bowel Diseases (IBDs). PLoS ONE *10*, e0125860.

35. Kermarrec, L., Eissa, N., Wang, H., Kapoor, K., Diarra, A., Gounni, A.S., Bernstein, C.N., and Ghia, J.E. (2019). Semaphorin-3E attenuates intestinal inflammation through the regulation of the communication between splenic $CD11C^{+}$ and $CD4^{+}$ $CD25^{-}$ T-cells. Br. J. Pharmacol. *176*, 1235–1250.

36. Meehan, T.F., Witherden, D.A., Kim, C.H., Sendaydiego, K., Ye, I., Garijo, O., Komori, H.K., Kumanogoh, A., Kikutani, H., Eckmann, L., and Havran, W.L. (2014). Protection against colitis by CD100-dependent modulation of intraepithelial γδ T lymphocyte function. Mucosal Immunol. *7*, 134–142.

37. Kang, S., Okuno, T., Takegahara, N., Takamatsu, H., Nojima, S., Kimura, T., Yoshida, Y., Ito, D., Ohmae, S., You, D.J., et al. (2012). Intestinal epithelial cell-derived semaphorin 7A negatively regulates development of colitis via αvβ1 integrin. J. Immunol. *188*, 1108–1116.

38. Pasterkamp, R.J., Peschon, J.J., Spriggs, M.K., and Kolodkin, A.L. (2003). Semaphorin 7A promotes axon outgrowth through integrins and MAPKs. Nature *424*, 398–405.

39. Suzuki, K., Okuno, T., Yamamoto, M., Pasterkamp, R.J., Takegahara, N., Takamatsu, H., Kitao, T., Takagi, J., Rennert, P.D., Kolodkin, A.L., et al. (2007). Semaphorin 7A initiates T-cell-mediated inflammatory responses through alpha1beta1 integrin. Nature *446*, 680–684.

40. Lang, R., Patel, D., Morris, J.J., Rutschman, R.L., and Murray, P.J. (2002). Shaping gene expression in activated and resting primary macrophages by IL-10. J. Immunol. *169*, 2253–2263.

41. Sordi, V., Malosio, M.L., Marchesi, F., Mercalli, A., Melzi, R., Giordano, T., Belmonte, N., Ferrari, G., Leone, B.E., Bertuzzi, F., et al. (2005). Bone marrow mesenchymal stem cells express a restricted set of functionally active chemokine receptors capable of promoting migration to pancreatic islets. Blood *106*, 419–427.

42. Wang, J., Zhang, W., He, G.H., Wu, B., and Chen, S. (2018). Transfection with CXCR4 potentiates homing of mesenchymal stem cells *in vitro* and therapy of diabetic retinopathy *in vivo*. Int. J. Ophthalmol. *11*, 766–772.

43. Fu, Y., Ni, J., Chen, J., Ma, G., Zhao, M., Zhu, S., Shi, T., Zhu, J., Huang, Z., Zhang, J., and Chen, J. (2020). Dual-Functionalized MSCs that Express CX3CR1 and IL-25 Exhibit Enhanced Therapeutic Effects on Inflammatory Bowel Disease. Mol. Ther. *28*, 1214–1228.

44. Sala, E., Genua, M., Petti, L., Anselmo, A., Arena, V., Cibella, J., Zanotti, L., D'Alessio, S., Scaldaferri, F., Luca, G., et al. (2015). Mesenchymal Stem Cells Reduce Colitis in Mice via Release of TSG6, Independently of Their Localization to the Intestine. Gastroenterology *149*, 163–176.e20.

45. Watanabe, S., Arimura, Y., Nagaishi, K., Isshiki, H., Onodera, K., Nasuno, M., Yamashita, K., Idogawa, M., Naishiro, Y., Murata, M., et al. (2014). Conditioned mesenchymal stem cells produce pleiotropic gut trophic factors. J. Gastroenterol. *49*, 270–282.

46. Karp, J.M., and Leng Teo, G.S. (2009). Mesenchymal stem cell homing: the devil is in the details. Cell Stem Cell *4*, 206–216.

47. Caplan, H., Olson, S.D., Kumar, A., George, M., Prabhakara, K.S., Wenzel, P., Bedi, S., Toledano-Furman, N.E., Triolo, F., Kamhieh-Milz, J., et al. (2019). Mesenchymal Stromal Cell Therapeutic Delivery: Translational Challenges to Clinical Application. Front. Immunol. *10*, 1645.

48. Ryser, M.F., Ugarte, F., Thieme, S., Bornhäuser, M., Roesen-Wolff, A., Brenner, S., et al. (2008). mRNA transfection of CXCR4-GFP fusion–simply generated by PCR-results in efficient migration of primary human mesenchymal stem cells. Tissue Eng Part C Methods *14*, 179–184.

49. Levy, O., Zhao, W., Mortensen, L.J., Leblanc, S., Tsang, K., Fu, M., Phillips, J.A., Sagar, V., Anandakumaran, P., Ngai, J., et al. (2013). mRNA-engineered mesenchymal stem cells for targeted delivery of interleukin-10 to sites of inflammation. Blood *122*, e23–e32.

50. Eissa, N., Hussein, H., Diarra, A., Elgazzar, O., Gounni, A.S., Bernstein, C.N., and Ghia, J.E. (2019). Semaphorin 3E regulates apoptosis in the intestinal epithelium during the development of colitis. Biochem. Pharmacol. *166*, 264–273.

51. Wirtz, S., Neufert, C., Weigmann, B., and Neurath, M.F. (2007). Chemically induced mouse models of intestinal inflammation. Nat. Protoc. *2*, 541–546.

52. Peng, Y., Chen, X., Liu, Q., Zhang, X., Huang, K., Liu, L., Li, H., Zhou, M., Huang, F., Fan, Z., et al. (2015). Mesenchymal stromal cells infusions improve refractory chronic graft versus host disease through an increase of CD5+ regulatory B cells producing interleukin 10. Leukemia *29*, 636–646.

53. Salero, E., Blenkinsop, T.A., Corneo, B., Harris, A., Rabin, D., Stern, J.H., and Temple, S. (2012). Adult human RPE can be activated into a multipotent stem cell that produces mesenchymal derivatives. Cell Stem Cell *10*, 88–95.

54. Ke, H., Wang, P., Yu, W., Liu, X., Liu, C., Yang, F., Mao, F.F., Zhang, L., Zhang, X., Lahn, B.T., and Xiang, A.P. (2009). Derivation, characterization and gene modification of cynomolgus monkey mesenchymal stem cells. Differentiation *77*, 256–262.

55. Pinho, S., Lacombe, J., Hanoun, M., Mizoguchi, T., Bruns, I., Kunisaki, Y., and Frenette, P.S. (2013). PDGFRα and CD51 mark human nestin+ sphere-forming mesenchymal stem cells capable of hematopoietic progenitor cell expansion. J. Exp. Med. *210*, 1351–1367.

56. Godoi, D.F., Cardoso, C.R., Ferraz, D.B., Provinciatto, P.R., Cunha, F.Q., Silva, J.S., and Voltarelli, J.C. (2010). Hematopoietic SCT modulates gut inflammation in experimental inflammatory bowel disease. Bone Marrow Transplant. *45*, 1562–1571.

57. González, M.A., Gonzalez-Rey, E., Rico, L., Büscher, D., and Delgado, M. (2009). Adipose-derived mesenchymal stem cells alleviate experimental colitis by inhibiting inflammatory and autoimmune responses. Gastroenterology *136*, 978–989.

58. Qin, A., Lai, D.H., Liu, Q., Huang, W., Wu, Y.P., Chen, X., Yan, S., Xia, H., Hide, G., Lun, Z.R., et al. (2017). Guanylate-binding protein 1 (GBP1) contributes to the immunity of human mesenchymal stromal cells against Toxoplasma gondii. Proc. Natl. Acad. Sci. USA *114*, 1365–1370.